



Article Processing Dates: Received on 2024-06-19, Reviewed on 2024-10-10, Revised on 2024-10-17, Accepted on 2024-10-19 and Available online on 2024-10-30

Shear strength comparison of single lap and joggle lap adhesive joints in carbon fiber composites manufactured via vacuum-assisted resin infusion

Mikhael Gilang Pribadi Putra Pratama*, Kosim Abdurohman, Rezky Agung Pratomo, Ryan Hidayat, Redha Akbar Ramadhan, Rian Suari Arintonang, Taufiq Satrio Nurtiasto, Riki Ardiansyah, Afid Nugroho, Awang Rahmadi Nuranto, Fajar Ari Wandono, Dudi Targani, Nur Mufidatul Ula

Research Center for Aeronautics Technology, Aeronautics and Space Research Organization, National Research and Innovation Agency, Bogor Regency, 16350, Indonesia

*Corresponding author: mikh001@brin.go.id

Abstract

The extensive utilization of composite materials has spurred the advancement of diverse joining techniques suitable for components constructed from such materials. This study focuses on the examination of two specific types of joints: single lap and joggle lap joints. The specimens utilized were composed of unidirectional carbon fiber composite combined with vinyl ester resin, manufactured via the vacuum-assisted resin infusion method. Vinyl ester adhesives were employed in the bonding process, with the joint surfaces undergoing sanding treatment prior to testing. Mechanical testing was conducted on the specimens according to ASTM D5868 standard, employing a constant crosshead speed until failure occurred. The test results reveal that the shear strength of single lap joints surpasses that of joggle lap joints. Within the single lap joint configuration, a mixed failure mode comprising both adhesive and cohesive failure is observed. Conversely, in joggle lap joints, substrate delamination is prevalent, suggesting the predominance of peel stress during loading.

Keywords:

Single lap joint, joggle joint, composite, shear strength.

1 Introduction

Carbon composites are lightweight structural materials characterized by a high stiffness-to-weight ratio, which makes them highly desirable for the aerospace, maritime, and automotive industries that require strong yet lightweight structures [1], [2], [3], [4], [5], [6]. The adoption of composite materials is increasingly replacing steel and aluminum in sectors such as marine, military, automotive, wind power generation, sports equipment, and construction [6], [7], [8], [9]. However, composite materials exhibit certain weaknesses, particularly low fracture toughness [10].

The diverse applications of composite materials have prompted the development of various bonding techniques applicable to components made from these materials [6]. Within the realm of composite materials, three types of joints are commonly identified: mechanical joints, adhesive joints, and hybrid joints that combine both types [11], [12]. Adhesive joints are progressively replacing mechanical joints due to their superior corrosion and fatigue resistance, elimination of the need for holes,

capability to distribute loads over a broader surface area, and reduced weight [6], [13], [14], [15]. Nonetheless, adhesive joints present several drawbacks, including the challenges associated with disassembling joints for inspection and repair, the necessity for meticulous surface preparation of adherends, and sensitivity to environmental conditions during operation [15]. Among the most significant challenges concerning the application of composite adhesive joints in the aerospace industry are their weak fracture toughness and low durability under harsh environmental conditions [10], [16].

The thickness, peel stress, and shear stress of the adhesive used are factors that influence the strength of adhesive joints [17]. The effectiveness of adhesive joints also depends on various other factors such as surface treatment of adherends, curing process, adhesive polymer composition, and chemical bonding between the adhesive and adherends [18]. Broadly speaking, adhesive joint failures can be categorized into three modes: adhesive failure mode, cohesive failure mode, and substrate failure mode [19], [20]. Adhesive failure mode occurs when the adhesive layer separates from the adherend, while cohesive failure mode occurs when the adhesive layer itself fails [20]. Substrate failure mode occurs when there is fiber breakage in the failure area [21].

Various studies have been conducted on the performance of single lap and joggle lap joints. One study examined the effects of various adhesive film curing methods on the performance of single-lap joint composites, with a specific focus on the impact of bond deficiencies [22]. Another investigation assessed the failure loads of composite single lap adhesive joints subjected to tensile and compressive loading [23]. Additionally, shear testing and acoustic emission testing were employed in a separate study to evaluate the bonding characteristics of single-lap and joggle-lap joints [17].

While previous research has provided valuable insights into the characteristics of adhesively bonded single-lap and joggle-lap joints, a gap remains in understanding their performance when fabricated using the Vacuum-Assisted Resin Infusion (VARI) method and utilizing the same matrix material as the adhesive. This study aims to address that gap by examining the influence of joint types on shear strength under these conditions. The controlled variables in this study included material type, surface treatment, and manufacturing method. The joint types investigated were single lap adhesive joints and joggle lap adhesive joints. The adherends used were carbon composites with a vinyl ester matrix, and the adhesive employed was also vinyl ester. Specimens were fabricated using the VARI method and tested according to ASTM D5868 standards.

2 Research Methodology

Fig. 1 outlines the key steps of this research. The process began with fabricating composite panels for the adherends and testing tabs, followed by cutting and sanding them to the required specifications. Adhesive was then applied to the prepared surfaces, and the adherends were joined. After curing, the specimens underwent mechanical testing in accordance with ASTM D5868, and the results were analyzed for failure modes.

2.1 Material and Composite Specimen Manufacturing

The adherend used in this study was a carbon composite consisting of 12 layers of unidirectional carbon fibers (0° orientation) and a vinyl ester matrix named Ripoxy R-800 EX-VI. The adherend was manufactured by creating a composite panel using the Vacuum-Assisted Resin Infusion (VARI) method with a 0.3% cobalt P-EX promoter and a 1% cumene hydroperoxide solution Percumyl-H catalyst. Other materials used in the manufacturing process included release agent, adhesive paper tape, sealant tape, peel ply, mesh ply, VARI plastic, resin hoses, spiral hoses, T connectors, resin containers, and a stirrer. The adhesive used for bonding in the adhesive joints was vinyl ester. All materials were purchased from Justus Kimia Raya, Indonesia.

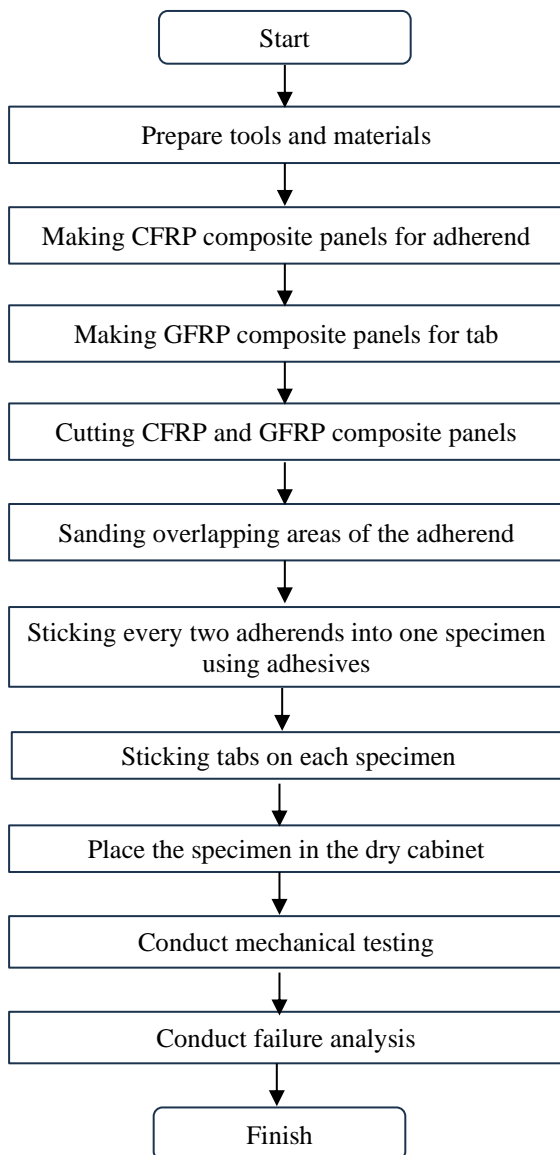


Fig. 1. Research flowchart.

The manufacturing process of the composite using the Vacuum-Assisted Resin Infusion (VARI) method involved several steps. The first step was to prepare all materials and tools required for the VARI process. The subsequent step entailed cleaning the mold, a glass table, to remove any dirt and applying a release agent to facilitate the easy demolding of the dried composite panel. Following this, sealant tape was applied around the lamination area, and resin inlet hoses, resin outlet hoses, and spiral hoses were installed. Dry composite fiber sheets were then placed in the lamination area on the glass mold, covered with peel ply, mesh ply, and bagging plastic to create an airtight seal. The air in the lamination area was evacuated using a vacuum pump. The next step involved checking for leaks by turning off the vacuum pump and monitoring the needle on the pressure gauge, as well as employing a leak detector to inspect the lamination area. Leakage could be identified by a drop in the needle on the pressure gauge or by detecting sound through the leak detector. Once the vacuum conditions were established, the resin and promoter were mixed and stirred at 500 rpm for one minute using a stirrer. Hardener was then added to the resin-promoter mixture and stirred until homogeneous using the same procedure. The mixed resin with promoter and hardener was subsequently flowed through the inlet channels to wet all parts of the composite fiber. The vacuum pump continued to operate until the resin cured, maintaining a vacuum pressure of 100 kPa throughout the process. The composite panel was left to cure at room temperature for 24 hours (Fig. 2). The vacuum pump utilized was the Vacmobile vacuum pump from New Zealand.

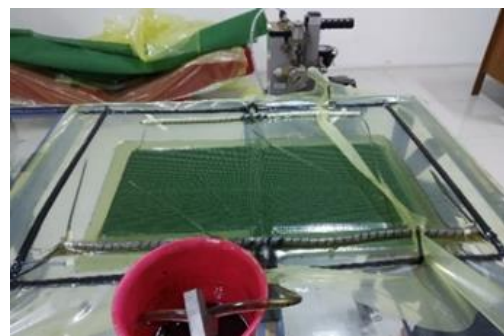


Fig. 2. Composite panel manufacturing setup.

The composite panels for the single lap and joggle lap joint specimens were fabricated using a glass table mold. The single lap composite panel was constructed flat (Fig. 3(a)), while the joggle lap incorporated a joggle at one end of the panel (Fig. 3(b)), achieved by attaching a 2 mm thick balsa core coated with plastic to the glass table mold. The joggle at the end of the composite measured 25.4 mm in length. The adherends were produced by cutting the cured composite panels with a waterjet cutting machine (Fig. 3(c)), resulting in dimensions of 101.6 mm × 25.4 mm in accordance with ASTM D5868. The 25.4 mm × 25.4 mm areas designated for bonding on each adherend were sanded using a Rockwell sanding machine equipped with an 800-grit sandpaper belt (Fig. 3(d)).

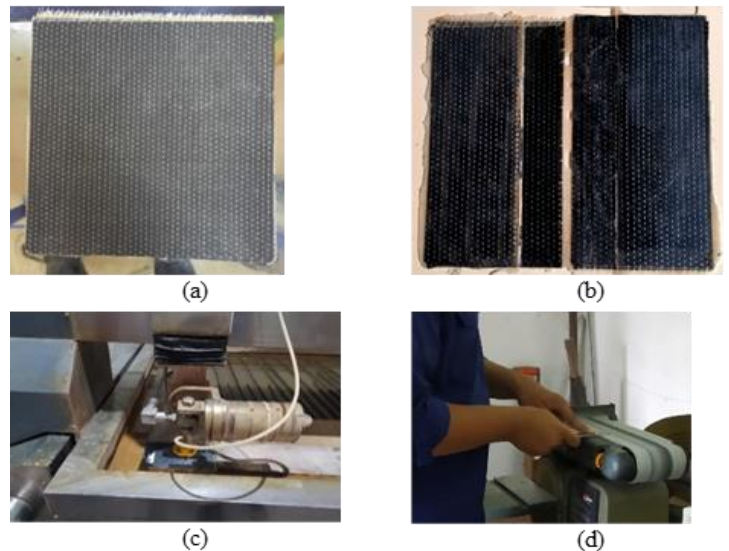


Fig. 3. (a) Single lap composite panel, (b) joggle lap composite panel, (c) waterjet cutting, and (d) adherend sanding.

The specimens were created by bonding two adherends using vinyl ester adhesive with an overlap length of 25.4 mm. The overlap area was clamped using paper clips, and excess adhesive that oozed out due to pressure was cleaned using a dry cloth. The specimens were then left to cure for 24 hours at room temperature until the adhesive fully cured.

A total of 5 specimens were created for both single lap and joggle lap joints. After the joints were assembled, they were placed inside a dry cabinet with a temperature of $23 \pm 2^\circ\text{C}$ and a humidity of $50 \pm 5\%$ RH for a minimum of 40 hours. This ensured that the joints were properly cured and acclimatized to the testing environment before conducting any further testing or analysis. The design of the joints can be seen in Fig. 4.

On the single lap joint specimen, tabs were installed at both ends. These tabs were installed to ensure that the load during testing is applied directly to the specimen. The tabs were made of e-glass/vinyl ester composite produced using the hand lay-up method. The dimensions of the tab were 25.4 mm × 25.4 mm, and they were attached to the specimen using vinyl ester adhesive. An illustration of the specimen with tabs installed as shown in Fig. 5.

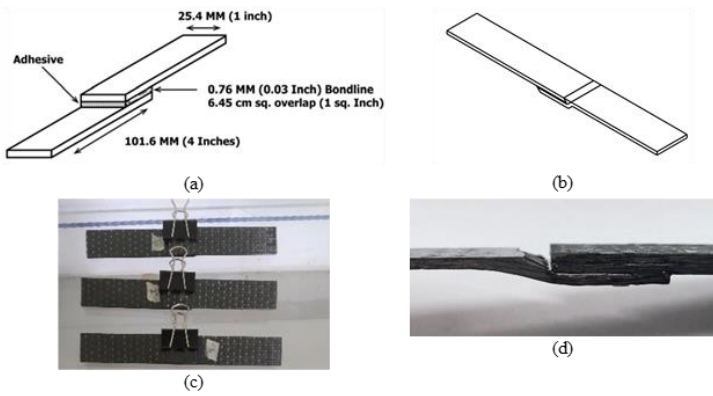


Fig. 4. (a) Single lap composite joint design, (b) joggle lap joint design, (c) bonding of single lap joint specimen, and (d) joggle lap joint specimen.

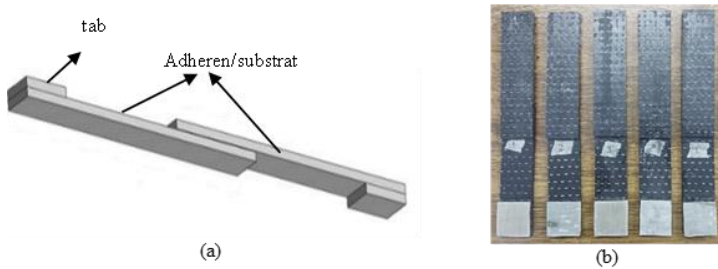


Fig. 5. (a) Illustration of the single lap joint specimen with tabs and (b) the specimen with tabs installed.

2.2 Testing Method

The testing method employed in this study was the single-lap shear adhesion test based on ASTM D5868. The tests were conducted using the UTM Tensilon testing machine from AND Japan with a capacity of 100 kN (Fig. 6) and a pull rate of 13 mm/minute. The testing environment maintained a temperature of $23\pm 2^{\circ}\text{C}$ and a humidity level of $50\pm 5\% \text{RH}$. Specimens were tested until failure occurred either at the adherend or at the joint. Load data and strength were recorded using UTM software. All testing procedures were carried out at the Material Testing Laboratory of the Aviation Technology Research Center, BRIN.

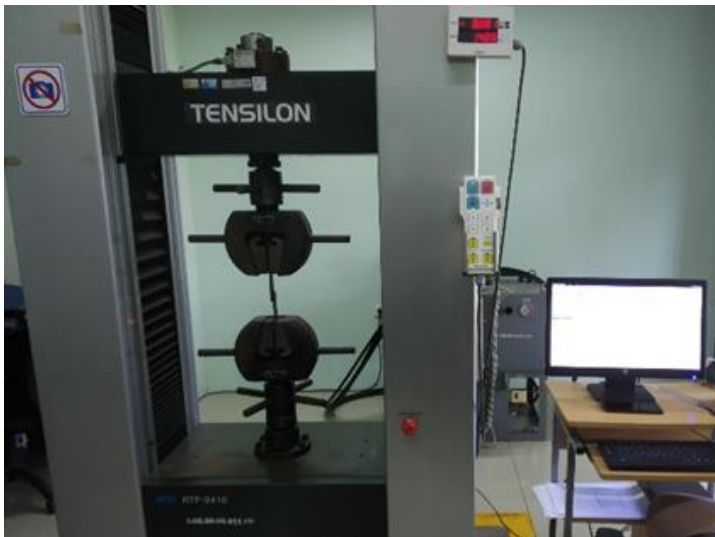


Fig. 6. Testing setup.

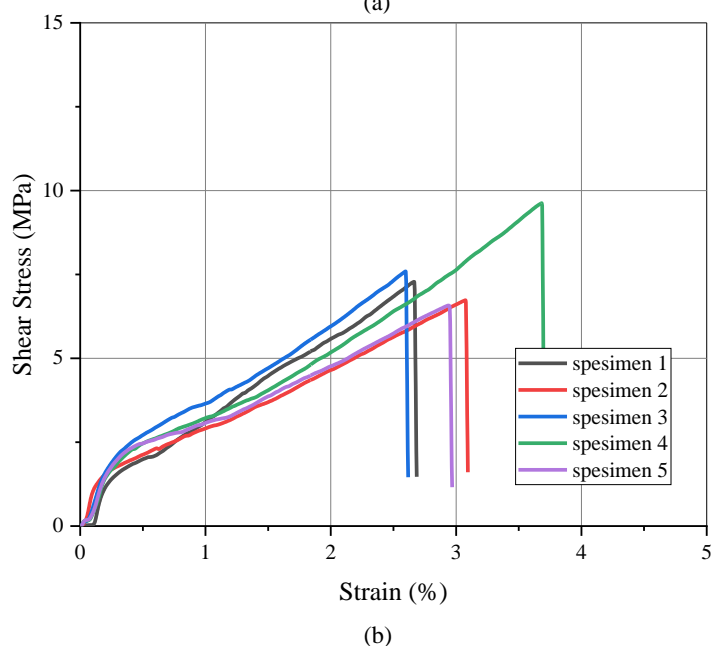
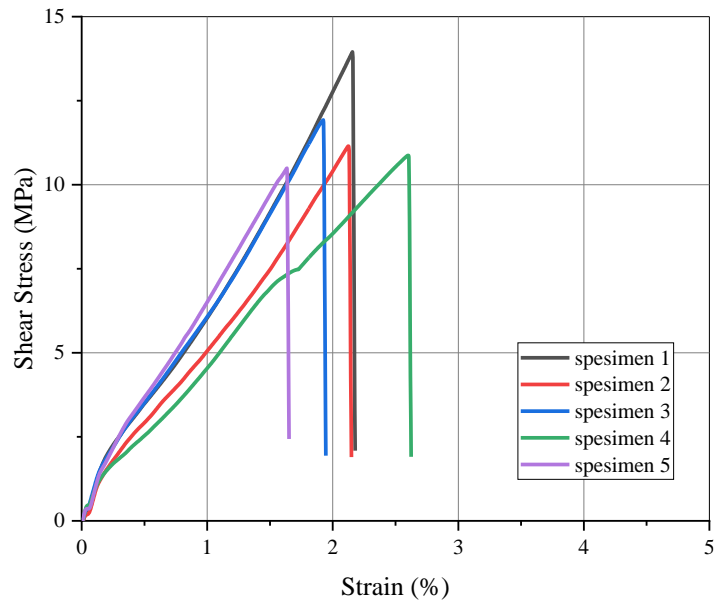
2.3 Fracture Surface Observation

Fracture observations of the joints in this study were conducted on specimens after testing. These observations were performed to determine the failure mode of the joints and the load transfer mechanism that occurred. In this research, the fractures of both joint types were photographed using a camera and a digital microscope to obtain images with clear detail. The photography was carried out at the Aerostructure Building, Aviation Technology Research Center, BRIN.

3 Results and Discussion

3.1 Joint Test Results

The primary results were presented alongside the analysis. Fig. 7 illustrates the stress versus strain graph derived from testing unidirectional carbon fiber composite single lap and joggle lap joint specimens. The test results indicated differences in the characteristics of the graphs for the single lap and joggle lap specimens. Both graphs exhibited distinct slopes, signifying differences in stiffness. The slope of the single lap graph was steeper than that of the joggle lap, as shown in Fig. 7(a), indicating that the single lap specimen was stiffer than the joggle lap specimen. Conversely, the slope of the joggle lap specimen graph was lower than that of the single lap specimen, as depicted in Fig. 7(b), suggesting reduced stiffness. Additionally, the maximum shear stress values for both specimens varied, as illustrated in Fig. 7(c). The maximum shear stress of the single lap specimen ranged from 10 MPa to 15 MPa, while that of the joggle lap specimen ranged from 5 MPa to 10 MPa. Differences in the graphs of both specimens were also observed in their strain values. The maximum strain of the single lap composite specimen ranged from 2% to 4%, whereas the maximum strain of the joggle lap specimen ranged from 3% to 4%. These results indicate that the single lap joint specimen exhibited greater stiffness and shear strength compared to the joggle lap joint specimen. Specimens with higher stiffness demonstrated lower strain, and vice versa.



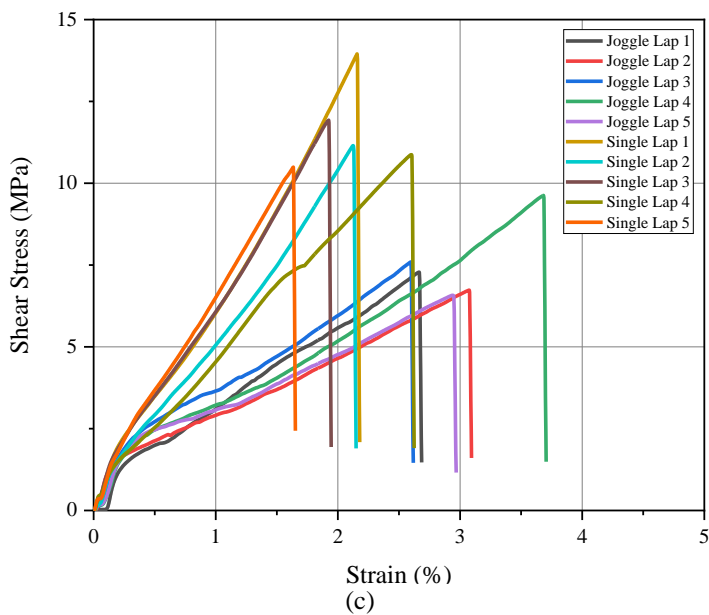


Fig. 7. (a) The stress vs. strain graphs resulting from the testing of single lap, (b) joggle lap joints, and (c) the combined graph.

Single lap joints primarily transmit forces through shear mechanisms when subjected to loads, while joggle lap joints primarily transmit forces through peel mechanisms [17]. This observation is consistent with the research findings and may explain the lower shear strength of joggle lap joints.

Fig. 8 presents the shear strength values of carbon composite adhesive joints for both single lap and joggle lap configurations. The shear strength of single lap carbon composite adhesive joints was measured at 11.68 ± 1.37 MPa, in contrast to 7.56 ± 1.23 MPa for joggle lap joints. This indicates that the shear strength of single lap carbon composite adhesive joints is 54% higher than that of joggle lap joints. These results should be considered in the application of carbon composite adhesive joint structures. In addition to strength values, the final product outcomes must also be taken into account when selecting joint applications. If the primary consideration is strength, single lap adhesive joints may be preferred. However, if the final product necessitates a smooth structural surface, joggle lap adhesive joints may be favored, particularly when filler is added to the joint gap.

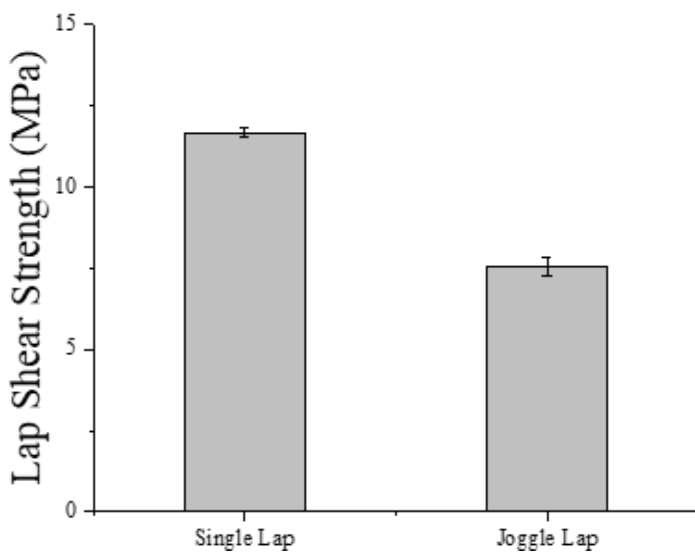


Fig. 8. The shear strength of carbon composite adhesive joints.

3.2 Observation of Joints Fracture Surface

Observations were conducted on the surface images of the fractures of single lap and joggle lap joints, as depicted in Fig. 9 and Fig. 10.

Fig. 9 illustrates that one substrate features areas devoid of adhesive layers, while the other substrate displays regions where

the adhesive remains intact, as well as clear indications of adhesive fractures. This observation suggests a mixed mode of failure, encompassing both adhesive and cohesive failure. The adhesive failure mode occurs at the adhesive/substrate interface, characterized by the adhesive detaching from one substrate and adhering to the other. Conversely, cohesive failure transpires within the adhesive itself, as evidenced by the adhesive fractures. This failure mechanism arises from axial forces applied during testing, which initially induce adhesive fractures (cohesive failure), followed by the adhesive detaching from one substrate (adhesive failure) until the joint can no longer sustain the load. Additionally, Fig. 9 reveals a matrix layer fracture in the joint fracture area. The adhesive fractures exhibited brittleness, primarily influenced by axial forces, with minor peeling observed. Based on the conditions of the adhesive fracture, it is concluded that the predominant stress on the joint is shear stress, accompanied by a minor component of peel stress.

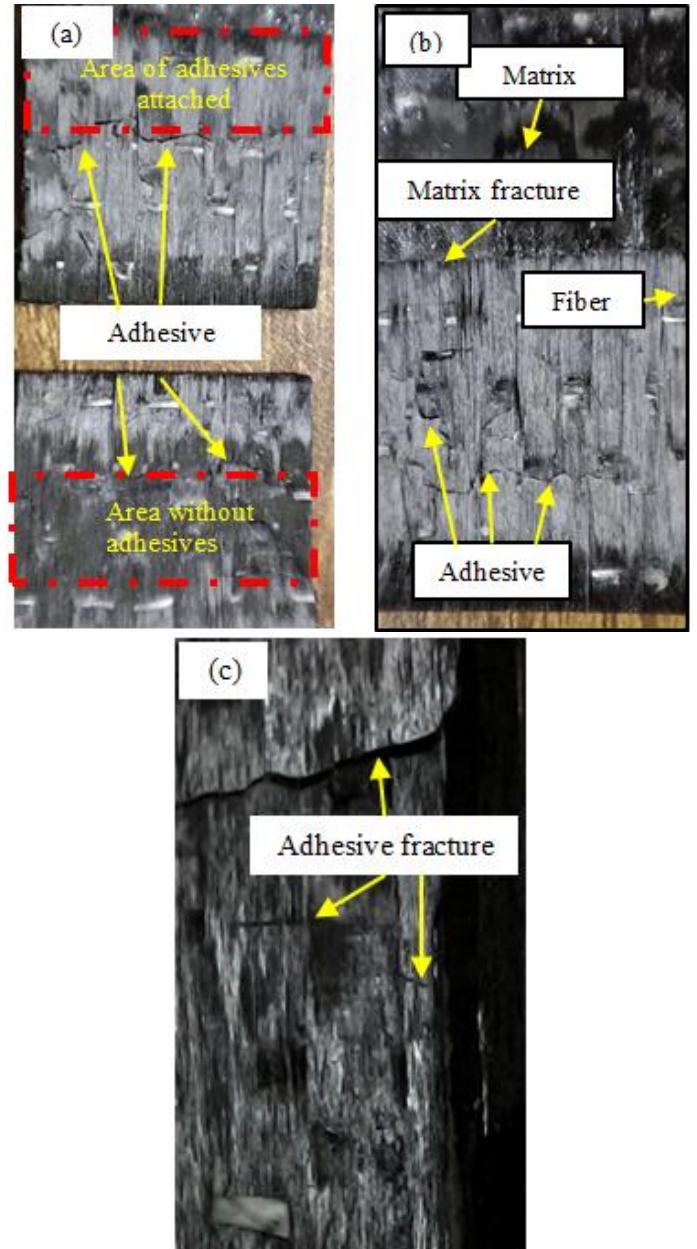


Fig. 9. Fracture images of the single lap joint type: (a) both sides of the joint fracture, (b) the fracture and non-fracture areas of the joint, (c) magnified image of the joint fracture.

In Fig. 10, it can be seen that the failure occurring at the joint location was dominated by delamination. The dominance of delamination damage indicates that the stress in that area was primarily peel stress. The presence of fiber delamination in the adherend indicates that the failure was a type of substrate failure.

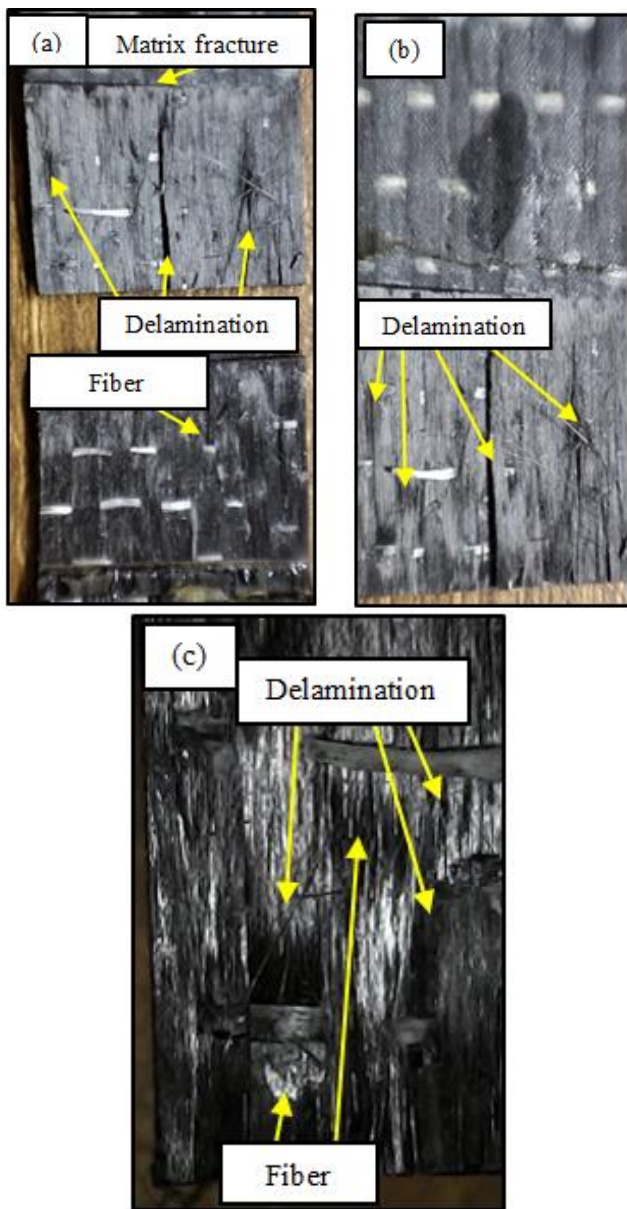


Fig. 10. Fracture images of the joggle joint type: (a) both sides of the joint fracture, (b) the fracture and non-fracture areas of the joint, (c) magnified image of the joint fracture.

Based on the observations of the fracture surface of the joint, the dominant stress in the single lap joint was shear stress, whereas the dominant stress in the joggle lap joint was peel stress. This phenomenon was consistent with the analysis of the test graphs and was a key factor in the difference in shear strength between single lap and joggle lap joints.

Mixed adhesive and cohesive failure occurred in the single lap joint, while substrate failure occurred in the joggle lap joint. The mixed failure mode occurred due to the good bonding of the adhesive, matrix, and composite fibers, as the adhesive type used was the same as the composite matrix. Substrate failure, indicated by delamination in the joggle lap joint, was mainly due to the peel stress that occurred during loading.

4 Conclusion

This study investigated the shear strength of adhesive joints in single-lap and joggle-lap configurations using unidirectional carbon fiber composites with a vinyl ester matrix, fabricated via the Vacuum-Assisted Resin Infusion (VARI) method. Experimental results demonstrated that single lap joints exhibited superior shear strength compared to joggle lap joints. The failure modes were distinct: single lap joints primarily displayed mixed failure, while joggle lap joints showed substrate failure. Fractographic analysis revealed predominant adhesive failure in the axial direction for single lap joints, whereas delamination was

more prominent in joggle lap joints. These observations suggest that the higher shear strength of single lap joints is due to the dominance of shear stresses, while peel stresses are the primary contributors to failure in joggle lap joints.

Acknowledgements

Through this statement, the authors would like to express gratitude for the library services and the research funding support from the Aerospace Research Organization No. 2/III.1/HK/2024 National Research and Innovation Agency-BRIN, Republic of Indonesia.

Contributorship Statement

MGPPP collected and analyzed the data and compiled the research article. KA conceived the idea, developed the methodology, and executed the experiment. RAP and RH manufactured the specimens and conducted the experiments. RAR provided theoretical assistance. RSA assisted in manufacturing the specimens and conducting the experiments. AN supplied the materials and supervised the specimen manufacturing. ARN and FAW contributed by addressing theoretical gaps. DT and NMU supervised the quality of specimen manufacturing.

References

- [1] F. Gnädinger, P. Middendorf, and B. Fox, "Interfacial shear strength studies of experimental carbon fibres, novel thermosetting polyurethane and epoxy matrices and bespoke sizing agents," *Compos Sci Technol*, vol. 133, pp. 104–110, 2016, doi: 10.1016/j.compscitech.2016.07.029.
- [2] G. Wu, L. Chen, and L. Liu, "Effects of silanization and silica enrichment of carbon fibers on interfacial properties of methylphenylsilicone resin composites," *Compos Part A Appl Sci Manuf*, vol. 98, pp. 159–165, 2017, doi: 10.1016/j.compositesa.2017.03.024.
- [3] N. K. Yadav, N. S. Rajput, S. Kulshreshtha, and M. K. Gupta, "Investigation of the Mechanical and Wear Properties of Epoxy Resin Composite (ERCs) Made With Nano Particle TiO₂ and Cotton Fiber Reinforcement," *Evergreen*, vol. 10, no. 1, pp. 63–77, 2023, doi: 10.5109/6781041.
- [4] S. Bindu, M. Prasanna Kumar, and K. M. Vinay, "Development and Mechanical Properties Evaluation of Basalt-Glass Hybrid Composites," *Evergreen*, vol. 10, no. 3, pp. 1341–1348, 2023, doi: 10.5109/7151681.
- [5] D. Choudhari and V. Kakhandki, "Characterization and Analysis of Mechanical Properties of Short Carbon Fiber Reinforced Polyamide66 Composites," *Evergreen*, vol. 8, no. 4, pp. 768–776, 2021, doi: 10.5109/4742120.
- [6] S. W. Park and D. G. Lee, "Adhesion strength of glass/epoxy composite embedded with heat-treated carbon black on the surface," *Compos Part A Appl Sci Manuf*, vol. 41, no. 11, pp. 1597–1604, 2010, doi: 10.1016/j.compositesa.2010.07.008.
- [7] D. S. Patil and M. M. Bhoomkar, "Investigation on Mechanical Behaviour of Fiber-Reinforced Advanced Polymer Composite Materials," *Evergreen*, vol. 10, no. 1, pp. 55–62, 2023, doi: 10.5109/6781040.
- [8] A. Anggoro Putra, D. Teguh Santoso, and F. Choria Suci, "Effect of Volume Fraction of Polyester Composite Reinforced Human Hair Fibers and Coconut Fibers On Mechanical Properties," vol. 20, no. 2, pp. 143–148, 2022, doi: 10.30811/jpl.v20i2.2935.
- [9] B. Istana, F. Alfredo, and S. Sunaryo, "Characterization of the Mechanical Properties of Fiberglass/Epoxy Prepreg Composites as Horizontal Axis Wind Turbine Blade Material: Influence of Fiber Orientation on Impact and Bending Strength," vol. 22, no. 4, pp. 457–461, 2024, doi: 10.30811/jpl.v22i4.5363.
- [10] M. Awi and A. S. Abdullah, "A Review on Mechanical Properties and Response of Fibre Metal Laminate under

- Impact Loading (Experiment),” *Evergreen*, vol. 10, no. 1, pp. 111–129, 2023, doi: 10.5109/6781057.
- [11] J. H. Kim, P. Lopez-Cruz, M. Heidari-Rarani, L. Lessard, and J. Laliberté, “An experimental study on the mechanical behaviour of bonded and hybrid bonded-bolted composite joints using digital image correlation (DIC) technique,” *Compos Struct*, vol. 276, no. March, p. 114544, 2021, doi: 10.1016/j.compstruct.2021.114544.
- [12] X. Li, Z. Tan, L. Wang, J. Zhang, Z. Xiao, and H. Luo, “Experimental investigations of bolted, adhesively bonded and hybrid bolted/bonded single-lap joints in composite laminates,” *Mater Today Commun*, vol. 24, no. May, p. 101244, 2020, doi: 10.1016/j.mtcomm.2020.101244.
- [13] G. Sinn *et al.*, “Mechanical and fracture mechanical properties of matrix-reinforced carbon fiber composites with carbon nanotubes,” *Key Eng Mater*, vol. 809 KEM, pp. 615–619, 2019, doi: 10.4028/www.scientific.net/KEM.809.615.
- [14] X. Cheng, J. Zhang, J. Bao, B. Zeng, Y. Cheng, and R. Hu, “Low-velocity impact performance and effect factor analysis of scarf-repaired composite laminates,” *Int J Impact Eng*, vol. 111, pp. 85–93, 2018, doi: 10.1016/j.ijimpeng.2017.09.004.
- [15] A. J. Kinloch, *Adhesion and Adhesives*, no. 1. 1987. [Online]. Available: <http://repositorio.unan.edu.ni/2986/1/5624.pdf> <http://fiskal.kemenkeu.go.id/ejournal> <http://dx.doi.org/10.1016/j.cirp.2016.06.001> <http://dx.doi.org/10.1016/j.powtec.2016.12.055> <https://doi.org/10.1016/j.ijfatigue.2019.02.006> <https://doi.org/10.1016/j.ijimpeng.2017.09.004>
- [16] C. Xiaoquan, Y. Manman, Z. Jie, Z. Qian, and Z. Jikui, “Thermal behavior and tensile properties of composite joints with bonded embedded metal plate under thermal circumstance,” *Compos B Eng*, vol. 99, pp. 340–347, 2016, doi: 10.1016/j.compositesb.2016.06.041.
- [17] C. Barile, C. Casavola, V. Moramarco, C. Pappalettere, and P. K. Vimalathithan, “Bonding characteristics of single-and joggled-lap CFRP specimens: Mechanical and acoustic investigations,” *Applied Sciences (Switzerland)*, vol. 10, no. 5, 2020, doi: 10.3390/app10051782.
- [18] X. Wei, H. Wang, and H. S. Shen, “A novel approach for the interfacial stress analysis of composite adhesively bonded joints,” *Compos Sci Technol*, vol. 184, no. September, p. 107830, 2019, doi: 10.1016/j.compscitech.2019.107830.
- [19] P. Yarrington, J. Zhang, C. Collier, and B. A. Bednarczyk, “Failure analysis of adhesively bonded composite joints,” *Collection of Technical Papers - AIAA/ASME/ASCE/AHS/ASC Structures, Structural Dynamics and Materials Conference*, vol. 10, no. April, pp. 6972–6994, 2005, doi: 10.2514/6.2005-2376.
- [20] A. Nemati Giv, Q. Fu, L. Yan, and B. Kasal, “Interfacial bond strength of epoxy and PUR adhesively bonded timber-concrete composite joints manufactured in dry and wet processes,” *Constr Build Mater*, vol. 311, no. July, p. 125356, 2021, doi: 10.1016/j.conbuildmat.2021.125356.
- [21] S. Omairey, N. Jayasree, and M. Kazilas, “Defects and uncertainties of adhesively bonded composite joints,” *SN Appl Sci*, vol. 3, no. 9, 2021, doi: 10.1007/s42452-021-04753-8.
- [22] R. Bhanushali, D. Ayre, and H. Y. Nezhad, “Tensile Response of Adhesively Bonded Composite-to-composite Single-lap Joints in the Presence of Bond Deficiency,” *Procedia CIRP*, vol. 59, no. TESConf 2016, pp. 139–143, 2017, doi: 10.1016/j.procir.2016.09.021.
- [23] M. Roy Choudhury and K. Debnath, “Experimental analysis of tensile and compressive failure load in single-lap adhesive joint of green composites,” *Int J Adhes Adhes*, vol. 99, no. November 2019, 2020, doi: 10.1016/j.ijadhadh.2020.102557.